



## Application of submerged plasma irradiation process for RNO treatment from an aqueous solution

Min Zhan<sup>a</sup>, Rahman Faizur Rafique<sup>a</sup>, Man Qi<sup>b</sup>, Gun Tae Son<sup>a</sup>, Seung Hwan Lee<sup>a,\*</sup>

<sup>a</sup>*School of Civil and Environmental Engineering, Kumoh National Institute of Technology, 1 Yangho-dong, Gumi, Gyeongbuk 730-701, Korea, emails: pobabyzhan@163.com (M. Zhan), dipu1219@gmail.com (R.F. Rafique), so20110@hanmail.net (G.T. Son), Tel. +82 10 9124 4240; email: dlee@kumoh.ac.kr (S.H. Lee)*

<sup>b</sup>*State Key Laboratory of Water Environment Simulation, School of Environment, Beijing Normal University, Beijing 100875, China, email: qiman@mail.bnu.edu.cn*

Received 17 December 2014; Accepted 3 May 2015

---

### ABSTRACT

This study attempted to remove an organic from an aqueous solution (wastewater) using submerged plasma irradiation (SPI) process. N, N-Dimethyl-4-nitrosoaniline (RNO) was used as a target material. Effect of electrode materials, applied voltage, initial concentration, and two types of buffer solutions were studied with the purpose of monitoring the pollutant removal. The degradation of RNO by SPI process followed a first-order kinetics model. While applying SPI, in comparison with the alkaline condition (carbonate buffer), the neutral condition (phosphate buffer) proved to be much more applicable in dealing with RNO contained by wastewater. After 8 min of operation, the removal efficiencies were found to be over 70% in the case of the carbonate buffer solution, and respectively 90% in the case of the phosphate one. By increasing the operation time and applied voltage, the SPI process had a significant effect on the pollutant removal. In comparison with the tungsten and aluminum electrodes, the iron one showed a higher efficiency in the removal process. Instead of using a high concentration pollutant in the initial stage, it was more beneficial to dilute the RNO wastewater before applying the SPI method.

*Keywords:* Submerged plasma irradiation; Decolorization; Buffer types; First-order kinetics model; Radicals

---

### 1. Introduction

Dye is a type of chemical product which is closely connected with peoples' daily lives; along with the rapid development of textile and apparel industry, the product's number of varieties increased as well [1]. In

recent years, with the application of new dyes, additives, chemical pulps, and finishing agents, the COD concentration in printing and dyeing wastewater also evolved from hundreds of mg/L to thousands of mg/L, which caused an increase in difficulty during processing and chromaticity removal [2]. As we know, most dyes have a high content of organic pollutants, refractory material, deep chromaticity, high alkalinity,

---

\*Corresponding author.

*Presented at the 7th International Conference on Challenges in Environmental Science and Engineering (CESE 2014) 12–16 October 2014, Johor Bahru, Malaysia*

complicated water quality change, and so on, which cannot be detected and degraded easily by the natural environment [3–5]. Therefore, the development of effective dye wastewater treatment technologies is becoming one of the most urgent and crucial tasks for researchers [6].

A lot of recent research is focusing on so-called advanced oxidation processes (AOPs), such as Fenton processes [7], ozone ( $O_3$ ) [8], hydrogen peroxide ( $H_2O_2$ ) and/or UV light [8,9], and photocatalysis [10]. AOPs, in a broad sense, refers to a set of chemical treatment procedures designed to remove organic (and sometimes inorganic) materials from water and wastewater by oxidation through reactions with hydroxyl radicals ( $OH^\bullet$ ) [11]. Non-thermal plasma generated by electrical discharges in liquid or at the gas–liquid interface leads also to the formation of oxidizing species: radicals ( $H^\bullet$ ,  $O^\bullet$ , and  $OH^\bullet$ ) and molecules ( $H_2O_2$ ,  $O_3$ , etc.), which are effective for the removal of pollutants [12]. This technology utilized in wastewater treatment attracts particular interest due to its excellent performance of attacking the organic pollutants and having no secondary pollution effects [6]. As a typical electrical discharge model, compared to other common AOPs, the primary benefit of plasma is its ability to generate UV light and oxidizing species, ozone, hydroxyl radicals, etc. without any chemical addition, or the use of UV lamps [13,14].

The aim of the present work is to understand the mechanism of plasma technology in dye wastewater treatment. In treating dye wastewater, namely N, N-dimethyl-4-nitrosoaniline (RNO) (Fig. 1), which is a typical basic mononuclear aromatic, part of the nitroso-group and the N-dimethyl-group, RNO is used quite frequently to measure the production of free

radicals formed during the electrochemical treatment, because RNO reacts rapidly and selectively with hydroxyl radicals [15]. Also, as a very toxic organic compound, when RNO has a higher concentration than normal in air or wastewater, it can lead to the occurrence of acute effects on health and also to the appearance of various environmental problems [16]. The bleaching of RNO solution by hydroxyl radicals is measured by absorbance changes at 440 nm [17]. This study attempted to remove an organic from an aqueous solution (wastewater) using submerged plasma irradiation (SPI) process. RNO was used as a target material. The purpose of the research was to investigate RNO solution absorbance reduction and to obtain optimal conditions for the process.

## 2. Materials and methods

### 2.1. Reagents

All chemicals used in this study were purchased from Daejung Chemicals & Metals Co., Ltd., Siheung-city, Gyeonggi-do, Korea, while the processing reagent RNO (Fig. 1) used in the experiments was purchased from Geel, Belgium, New Jersey, USA. Distilled water with a conductivity of less than 0.5 mS/m was used to prepare all solutions. RNO stock solution was dissolved in 100 mmol/L (15.018 g/L) of distilled water before use.

### 2.2. Apparatus

The schematic diagram of experimental apparatus is shown in Fig. 2. The pulsed electric discharge was generated in the electrode system of the needle-to-plane electrode geometry located in the center of a Plexiglas cylinder. The inner diameter and the height of the discharge reactor were 50 mm and 180 mm, respectively. The ground plate electrode was at the outside end at the bottom of the reactor. A pulsed power supply with a rotating spark gap switch was used to generate high voltage pulses. The pulse voltage was controlled with the value of output voltage in 0–2,000 V. The needle electrodes were made of iron, aluminum, and tungsten (after carefully analyzing the resistivity, conductivity, and the price of various other materials as well), each with a diameter of 2 mm and enclosed in a ceramic case.

### 2.3. Experimental design

During the experiment, the pulse voltage was set at 500, 600, 700, and 800 V, the operation time varied

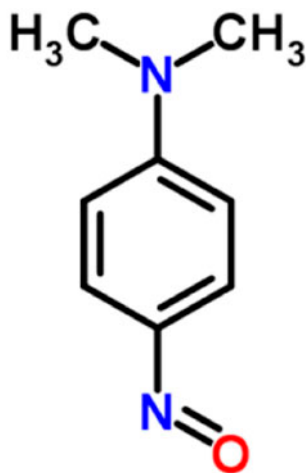


Fig. 1. Chemical structure of a RNO molecule.

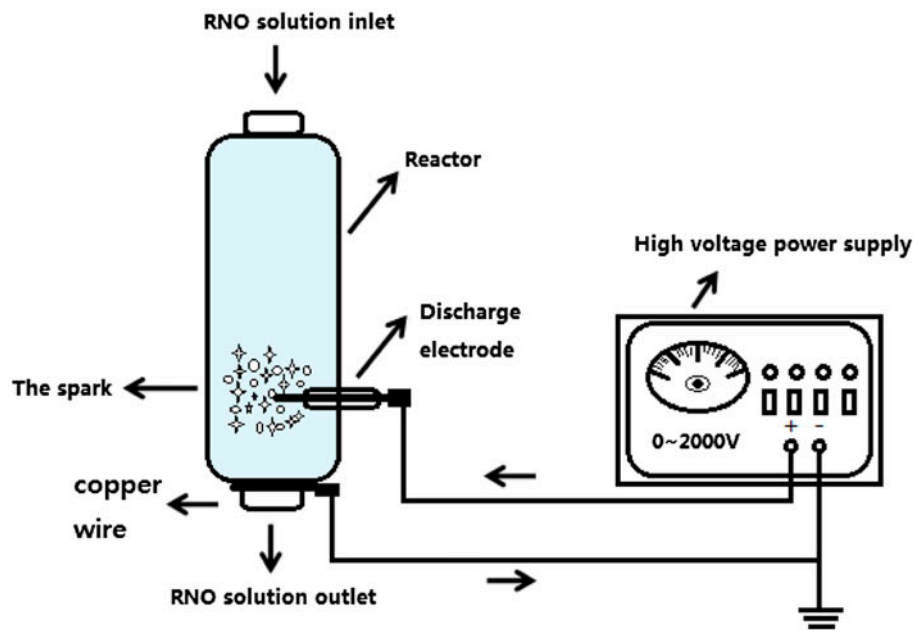


Fig. 2. Schematic diagram of experimental apparatus.

from 2 to 10 min, the materials of the needle electrodes were made of iron, tungsten, and aluminum, and the total volume of 50 mL of RNO solution with an initial concentration of 15, 37.5, and 75 mg/L circulated through the reactor; also, the original RNO solutions were diluted with two different buffers: carbonate buffer and phosphate. The details of the buffers were monitored as listed in Table 1.

#### 2.4. Measurement of decolorization efficiency

Samples were taken periodically from the reactor, and the concentrations of RNO solution were calculated by measuring the absorbencies of the solution analyzed immediately using HS-3300 spectrophotometer (HUMAS, Korea) with a wavelength of 440 nm [16]. The dye removal efficiency was calculated based on the following equation [18]:

$$\eta = \frac{\alpha_0 - \alpha_t}{\alpha_0} \times 100\% \quad (1)$$

where  $\alpha_0$  (mg/L) was the initial concentration and  $\alpha_t$  (mg/L) was the concentration at reaction time  $t$  (min).

#### 2.5. Kinetic study

The kinetics of RNO decolorization by applying SPI process under various reaction conditions was investigated. In the present study, zero-, first-, and second-order reaction kinetics were used to study the decolorization kinetics of RNO through SPI process. The expressions guiding the reaction kinetics are presented below:

Zero-order reaction kinetics:

$$d\alpha_t / dt = -k_0 \quad (2)$$

First-order reaction kinetics:

$$d\alpha_t / dt = -k_0\alpha_t \quad (3)$$

Table 1  
Analytical conditions for buffers

Buffer	Reagents	pH	Conductivity (mS/m)
Carbonate buffer	Na <sub>2</sub> CO <sub>3</sub> , NaHCO <sub>3</sub>	9.60 ± 0.02	8.13 ± 0.05
Phosphate buffer	Na <sub>2</sub> HPO <sub>4</sub> , NaH <sub>2</sub> PO <sub>4</sub>	6.70 ± 0.02	6.62 ± 0.05

Second-order reaction kinetics:

$$d\alpha_t / dt = -k_0\alpha_t^2 \quad (4)$$

where  $k_0$  ( $\text{mg/L min}^{-1}$ ),  $k_1$  ( $\text{min}^{-1}$ ) and  $k_2$  ( $\text{L/mg min}^{-1}$ ) represent the apparent kinetic rate constants of zero-, first-, and second-order reaction kinetics, and  $t$  is the reaction time [19].

Integrating Eqs. (2)–(4), the following equations were obtained:

$$\alpha_t = \alpha_0 - k_0t \quad (5)$$

$$\ln\left(\frac{\alpha_0}{\alpha_t}\right) = k_1t \quad (6)$$

$$\frac{1}{\alpha_t} - \frac{1}{\alpha_0} = k_2t \quad (7)$$

Regression analysis based on the zero-, first-, and second-order reaction kinetics for the decolorization of RNO using SPI process was conducted in order to investigate the reaction conditions which would best fit the process [20].

The  $G_{99\%}$  presents the energy efficiency of degradation process when the concentration of the target is reduced by 99% comparing to its initial concentration, and it can be estimated based on first-order kinetics as below [6,21]:

$$G[\text{g} / \text{kWh}] = \frac{\alpha_0 V \eta(\%)}{100Pt} \quad (8)$$

where  $\alpha_0$  ( $\text{mg/L}$ ) is the initial concentration of RNO,  $V$  ( $\text{L}$ ) is the total solution volume,  $P$  ( $\text{W}$ ) is input power, and  $t$  is reaction time.

### 3. Results and discussion

#### 3.1. Effect of reaction time and buffer conditions

The decolorization efficiency as a function of operation time is presented in Figs. 3–5; as it can be observed, along with the elapsing of time, regardless of the different electrodes or buffers used, the RNO decolorization efficiency also increased constantly. For example, in the beginning, before the operation time reached 4 min, the rate increased slowly and steadily, while after that time and until minute 6 of the operation the removal rate had a sharp growth; after 8 min, the removal efficiency growth started to slow down. As we know, the production of plasma through

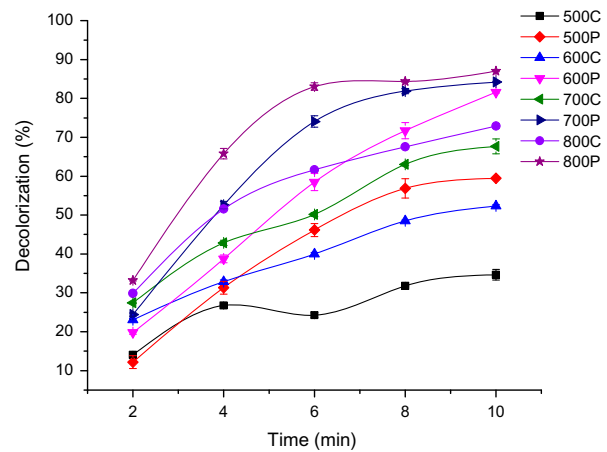


Fig. 3. Effect of buffer solutions on RNO degradation (conditions: buffers carbonate/C, phosphate/P; input voltage 500–800 V; electrode iron; initial concentration 75 mg/L; and operation time 2–10 min).

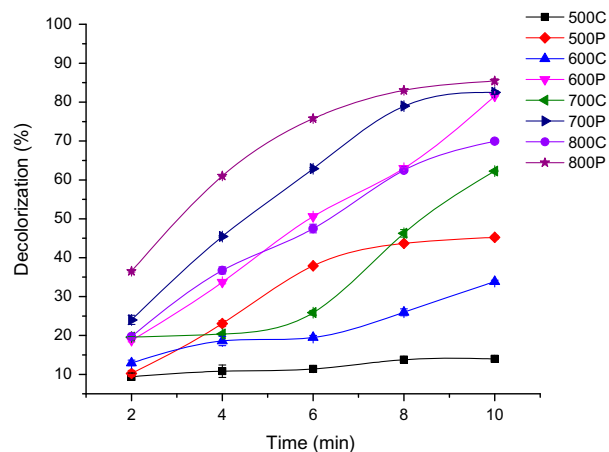


Fig. 4. Effect of buffer solutions on RNO degradation (conditions: buffers carbonate/C, phosphate/P; input voltage 500–800 V; electrode tungsten; initial concentration 75 mg/L; and operation time 2–10 min).

high voltage electric discharges involves a significant expense of energy, and it also is a time-consuming process. So, considering the SPI reaction time, it was recommended to increase the operation time [22].

Additionally, it is well known that the pH of wastewater can be found in a wide variety and that oxidation processes are very sensitive to the pH of aqueous solutions [23]. In this study, the usage of two different buffer solutions (carbonate buffer alkaline condition; phosphate buffer neutral condition) played a very important role in the RNO degradation. A high decolorization efficiency of aqueous RNO was obtained when using different buffer conditions, as

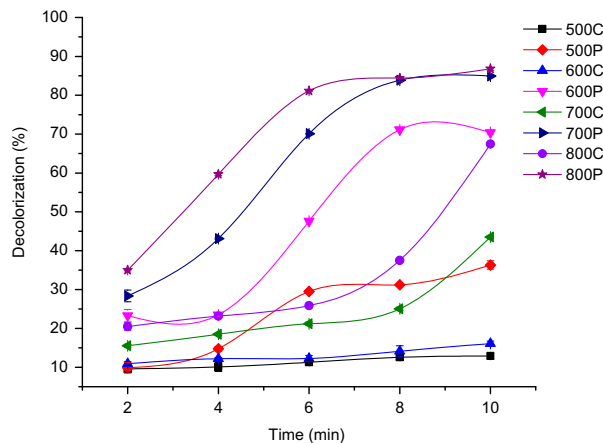


Fig. 5. Effect of buffer solutions on RNO degradation (conditions: buffers carbonate/C, phosphate/P; input voltage 500–800 V; electrode aluminum; initial concentration 75 mg/L; and operation time 2–10 min).

shown in Figs. 3–5; if comparing the carbonate buffer's experimental results with the phosphate buffer's results, significant differences between the two can be observed; overall, the phosphate buffer contributed to the RNO removal rate more efficiently than the carbonate buffer. Specifically, in the case of a long period of time and higher voltage discharges (8–10 min and 800 V), the removal rate reached almost 90% with the phosphate buffer, and 70% with the carbonate buffer. At the same time, when the period of elapsed time was longer, even if the voltage discharges were lower (500 V), the removal rates also showed a higher efficiency with phosphate buffer than with carbonate buffer (30–50%, respectively, 10–20%). However, for a short period of elapsed time (2–4 min), the differences between the two situations were not as significant. From here, we can easily understand that phosphate buffer is recommended when dealing with RNO wastewater. Carbonate buffer has a pH of around 10

(alkaline) and phosphate buffer has a pH of around 7 (neutral); also, if relating to results from other researchers, the plasma has better treatment efficiency in a neutral condition, because in an alkaline condition the chemicals can easily create other reactions aside from the production of plasma [24]. So we can easily understand why in the alkaline condition (carbonate buffer) the RNO could not be treated as efficiently as in the neutral condition (phosphate buffer); thus, it seemed to be more effective to rely on phosphate buffer as a condition when using plasma technology to deal with RNO wastewater.

In order to analyze the decolorization of RNO during the SPI process, the zero-, first-, and second-order reaction kinetics models were applied to the data. Regarding the values of the kinetic rate constants and the regression coefficients in different buffer conditions, the results (obtained at the optimum experimental conditions) of the regression analysis are shown in Table 2 as following: (a) the zero-order is in the range of 0.6574–0.9176 with an average of 0.8216; (b) the first-order is in the range of 0.8897–0.9858 with an average of 0.9613; and (c) the second-order is in the range of 0.8537–0.9720 with an average of 0.9045. These results indicate that the first-order reaction kinetics best describe the decolorization of the RNO through SPI process [20]. Likewise, the comparisons of the calculated results for the first-order kinetic model in two different buffer conditions also predicted that it is more efficient to remove RNO in a neutral condition (phosphate buffer) than in an alkaline condition (carbonate buffer), since the former kinetic rate constants are much higher than the second ones.

### 3.2. Effect of discharge voltage

To evaluate the energy efficiency improvement capacity of pulsed power supply, the efficiency of four different discharge voltages were also tested during

Table 2  
Comparisons of kinetic rate constants via various discharge voltages and buffer conditions for RNO decolorization

Voltage	Buffer conditions	Initial concentration (mg/L)	Electrode materials	Zero-order		First-order		Second-order	
				$k_0$ (mg/L min <sup>-1</sup> )	$R^2$	$k_1$ (min <sup>-1</sup> )	$R^2$	$k_2$ (L/mg min <sup>-1</sup> )	$R^2$
500 V	Carbonate buffer	75	Iron	0.022	0.8592	0.040	0.8897	0.043	0.8613
600 V				0.037	0.7509	0.072	0.9589	0.056	0.9328
700 V				0.035	0.8690	0.112	0.9653	0.058	0.9399
800 V				0.050	0.8968	0.130	0.9702	0.056	0.9720
500 V	Phosphate buffer	75	Iron	0.082	0.6574	0.098	0.9699	0.243	0.8588
600 V				0.164	0.7788	0.171	0.9765	0.615	0.8537
700 V				0.369	0.8432	0.202	0.9747	0.877	0.8727
800 V				0.405	0.9176	0.218	0.9858	1.094	0.9450

the SPI process in this study [25,26]. As shown in Table 2, as the removal processes followed first-order kinetics, after plasma treatment, the kinetic rate constants for RNO degradation by 800 V voltage discharging (0.218 and 0.130 min<sup>-1</sup> for each buffer condition) were much larger than in the case of lower voltage discharging. In a similar direction, the regression coefficients for different discharge voltage conditions also dramatically differ from the large voltage situations to lower voltage ones (0.9702–0.8897 and, respectively, 0.9858–0.9699 for each buffer condition). Thus, it is believed that higher input voltage discharging displays a better decolorization efficiency than lower voltage discharging.

As pulsed power supply is an important factor that affects the decolorization efficiency of the plasma processes, another six different voltages were also tested to evaluate the energy efficiency for RNO decolorization. In Table 3, if comparing different pulsed power voltages used with plasma technology, the energy efficiency via 700–900 V (19.4–27.1 and 34.9–40.5 × 10<sup>-3</sup> g/kWh for each buffer condition) was much higher than other lower voltage discharges. Also, when comparing the different operation times, for 99% RNO removal efficiency, the 800 V voltage discharging was proved to have the best removal efficiency  $G_{99\%}$  in the shortest time. Thus, as shown in Table 3, among different pulsed power voltages, the

higher voltage discharges, especially the 800–900 V ones, seem to have a higher energy efficiency.

At the same time, in order to observe the differences in different experimental conditions, multiple comparisons were conducted. The outcomes are verified and validated by the experiment data, which confirms that a higher decolorization efficiency can be obtained as the input voltage is increased (Tables 4 and 5); more precisely, in carbonate buffer and phosphate buffer conditions, by increasing the discharging time, different voltages show significantly different decolorization efficiencies (in decreasing order): 800 > 700 > 600 > 500 V.

According to the results of different voltage discharges, the higher voltage discharge showed a very steady RNO decolorization efficiency; thus, it is recommended to apply a higher voltage when using plasma technology to deal with RNO wastewater.

### 3.3. Effect of initial concentration

In order to design a fast and effective model, further investigations into decolorization mechanism via different RNO initial concentrations were made. The decolorization efficiency as a function of treatment time with three different initial solutions is presented in Figs. 6–8. As it can be seen, the RNO decolorization efficiency decreased with the increase in initial

Table 3  
Comparison of energy efficiency via various discharge voltages and buffer conditions for RNO decolorization

Voltage	Carbonate buffer		Phosphate buffer	
	$G_{99\%}$ (10 <sup>-3</sup> g/kWh)	Time (min)	$G_{99\%}$ (10 <sup>-3</sup> g/kWh)	Time (min)
500 V	8.7	115.1	21.3	47.0
600 V	14.3	64.0	33.9	26.9
700 V	19.4	41.1	34.9	22.8
800 V	27.1	35.4	40.5	21.1
900 V	25.8	29.6	36.6	19.4
1000 V	25.3	26.4	38.8	15.2

Table 4  
Multiple comparisons of RNO decolorization efficiencies by increasing discharge voltage in carbonate buffer condition

Voltage	Discharge time				
	2 min	4 min	6 min	8 min	10 min
500 V	(11.0 ± 0.59)%	(15.9 ± 1.57)%	(15.6 ± 1.18)%	(19.4 ± 1.65)%	(20.5 ± 1.93)%
600 V	(15.6 ± 1.03)%	(21.2 ± 1.66)%	(23.9 ± 2.21)%	(29.6 ± 2.70)%	(34.1 ± 2.76)%
700 V	(20.8 ± 0.93)%	(27.2 ± 2.08)%	(32.4 ± 2.38)%	(44.8 ± 2.91)%	(57.8 ± 2.02)%
800 V	(23.4 ± 0.92)%	(37.2 ± 2.18)%	(45.0 ± 2.76)%	(55.8 ± 2.45)%	(70.1 ± 0.47)%

Table 5

Multiple comparisons of RNO decolorization efficiencies by increasing discharge voltage in phosphate buffer condition

Voltage	Discharge time				
	2 min	4 min	6 min	8 min	10 min
500 V	(10.8 ± 0.75)%	(23.0 ± 1.40)%	(37.9 ± 1.38)%	(43.9 ± 2.11)%	(47.0 ± 1.81)%
600 V	(20.6 ± 0.66)%	(32.0 ± 1.23)%	(52.2 ± 1.11)%	(68.6 ± 1.00)%	(77.9 ± 0.99)%
700 V	(25.6 ± 0.73)%	(47.0 ± 0.81)%	(69.0 ± 0.98)%	(81.6 ± 0.43)%	(83.9 ± 0.24)%
800 V	(34.9 ± 0.27)%	(62.2 ± 0.66)%	(78.0 ± 0.67)%	(83.9 ± 0.16)%	(86.4 ± 0.25)%

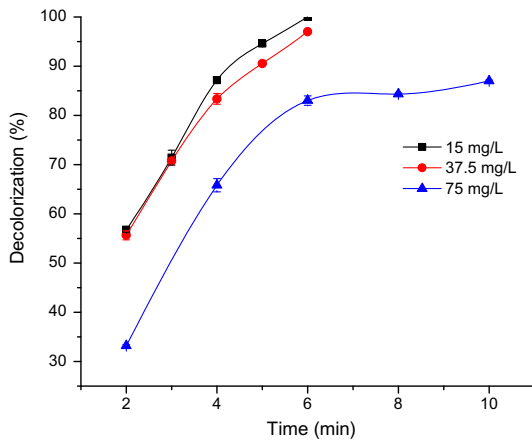


Fig. 6. Effect of initial concentration on RNO degradation (conditions: buffers phosphate/P; input voltage 800 V; electrode iron; and operation time 2–10 min).

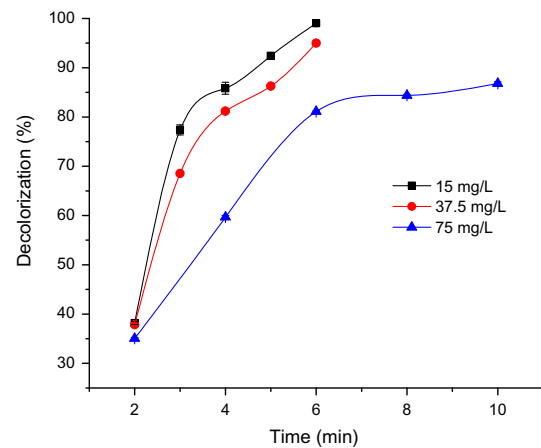


Fig. 8. Effect of initial concentration on RNO degradation (conditions: buffers phosphate/P; input voltage 800 V; electrode aluminum; and operation time 2–10 min).

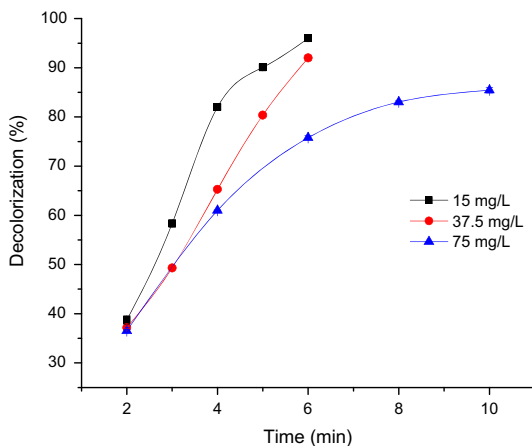


Fig. 7. Effect of initial concentration on RNO degradation (conditions: buffers phosphate/P; input voltage 800 V; electrode tungsten; and operation time 2–10 min).

solution concentration regardless of the type of electrode used. For example, for the initial 6 min of plasma treatment, the decolorization efficiency was

over 95% for 15 and 37.5 mg/L RNO solution, while, with a 75 mg/L initial concentration, samples only had an 80% removal rate. With a steady discharge, the active species produced in pulse discharge were maintained at specific concentration levels leading to a maximum degradation capability. After 6 min of plasma treatment, the decolorization efficiency reached only approximately 90% when increasing the initial concentration of RNO. With an extended operation time, instead of using a high initial concentration pollutant, it seemed more beneficial to dilute the RNO wastewater before applying the SPI process [27].

Similarly, another suitable method is proposed in order to better understand the mechanisms of the decolorization of RNO through the SPI process by using the zero-, first-, and second-order reaction kinetics models. The results of the regression analysis are shown in Table 5. With optimum experimental conditions, the values of the kinetic rate constants and the regression coefficients in different RNO initial concentrations through three different electrodes provided the following outcomes: (a) the zero-order was in the

range of 0.7358–0.9406 with an average of 0.9039; (b) the first-order was in the range of 0.9358–0.9920 with an average of 0.9680; and (c) the second-order was in the range of 0.7181–0.9575 with an average of 0.8001. These results indicate, once again, that the first-order reaction kinetics were the most appropriate for decolorization of RNO through the SPI process. Besides, in comparison with the calculated results in three different RNO initial concentrations via the first-order kinetic model, the lower initial concentration samples always reached better kinetic rate constants, which suggest that dilution is a very efficient measurement in the RNO decolorization process.

### 3.4. Effect of electrodes

According to other studies, the plasma is produced differently according to the change of electrode type [28]. Various electrodes were applied to study their effects on the degradation of RNO. As shown in Table 6, the results indicate that, with a first-order kinetic model, after plasma treatment, the kinetic rate constant for RNO degradation in lower and higher initial RNO concentration differs according to the electrode used (0.565, 0.468, and 0.436 min<sup>-1</sup>, for different electrodes). The regression coefficients in the case of

different electrode discharges also show the same results. Thus, after analyzing the various situations, it has been demonstrated that the iron electrode displays higher decolorization efficiency than the other two electrodes used.

Meanwhile, as it is shown in Tables 6 and 7, in carbonate buffer condition, the three different electrodes had a significant difference as well. The three electrodes showed three different removal efficiencies, as following (in decreasing order): iron > tungsten > aluminum. But, in the case of the phosphate buffer condition, the three electrodes presented different removal efficiencies when changing the discharge time: for a short discharge time (2 min), the aluminum electrode showed a more significant difference than the iron and the tungsten ones, while there seemed to be no obvious differences between the last two mentioned (iron and tungsten). When the discharge time was longer (over 2 min), the three electrodes showed similar removal efficiencies as in the carbonate buffer condition: iron > tungsten > aluminum [29].

According to the results obtained after using different electrodes, the iron electrode showed the steadiest RNO removal efficiency. Thus, also taking into consideration the fact that iron is a very common material, it can be stated that using an iron electrode

Table 6

Comparisons of kinetic rate constants via various initial concentration and electrode materials for RNO decolorization

Initial concentration (mg/L)	Electrode materials	Voltage	Buffer conditions	Zero-order		First-order		Second-order	
				$k_0$ (mg/L min <sup>-1</sup> )	$R^2$	$k_1$ (min <sup>-1</sup> )	$R^2$	$k_2$ (L/mg min <sup>-1</sup> )	$R^2$
15	Iron	800 V	Phosphate buffer	0.020	0.9406	0.565	0.9920	28.916	0.8537
37.5				0.045	0.9213	0.469	0.9808	7.204	0.8170
75				0.405	0.8432	0.218	0.9786	1.094	0.7181
15	Tungsten			0.019	0.9325	0.468	0.9813	17.008	0.9575
37.5				0.037	0.9513	0.312	0.9659	3.193	0.7650
75				0.039	0.7358	0.201	0.9358	1.301	0.7546
15	Aluminum			0.018	0.9449	0.436	0.9680	0.019	0.8353
37.5				0.044	0.9358	0.421	0.9531	5.255	0.8739
75				0.065	0.9301	0.215	0.9567	1.002	0.6261

Table 7

Multiple comparisons of RNO removal rate among 3 different electrodes in carbonate buffer condition

Electrode materials	Discharge time				
	2 min	4 min	6 min	8 min	10 min
Aluminum	(14.1 ± 0.77)%	(16.0 ± 0.89)%	(17.6 ± 1.02)%	(22.3 ± 1.64)%	(35.0 ± 3.56)%
Tungsten	(15.4 ± 0.76)%	(21.6 ± 1.60)%	(26.1 ± 2.17)%	(37.1 ± 3.01)%	(45.0 ± 3.59)%
Iron	(23.6 ± 0.98)%	(38.5 ± 1.53)%	(44.0 ± 2.21)%	(52.7 ± 2.24)%	(56.9 ± 2.46)%

Table 8

Multiple comparisons of RNO decolorization efficiencies among 3 different electrodes in phosphate buffer condition

Electrode materials	Discharge time				
	2 min	4 min	6 min	8 min	10 min
Aluminum	(24.1 ± 1.60)%	(35.3 ± 2.80)%	(57.1 ± 3.20)%	(67.6 ± 3.47)%	(69.6 ± 3.25)%
Tungsten	(22.4 ± 1.57)%	(40.8 ± 2.27)%	(56.8 ± 2.26)%	(67.2 ± 2.48)%	(73.7 ± 2.65)%
Iron	(22.4 ± 1.29)%	(47.1 ± 2.20)%	(65.4 ± 2.40)%	(73.7 ± 1.91)%	(78.1 ± 1.75)%

is the most efficient method while dealing with RNO wastewater through plasma technology.

#### 4. Conclusions

SPI process can effectively mineralize organic in aqueous solutions and is a viable alternative for the treatment of refractory organic pollutants in matter of fast removal rate and environmentally friendly. The process of RNO decolorization from water solutions has been investigated using three pulsed discharge modes in water. The decolorization process was complex and the active oxidation mechanisms were, most likely, hydroxyl radicals and ultraviolet light radiation. The degradation of RNO using the SPI process followed a first-order kinetics model. In the experimental system, electrode materials, applied voltage, initial concentration, and the type of buffer solutions were all important factors for RNO solution decolorization efficiency. Relatively high RNO removal efficiency was obtained in neutral condition (phosphate buffer). And, with the extension of operation time and the increase in applied voltage, more hydroxyl radicals were formed and reacted with RNO in the reaction system. The rise of initial concentration caused the decrease in the apparent kinetic rate constant. At the same time, as a very common material, the iron electrode was found to be the most efficient in removing RNO wastewater through the SPI process.

#### Acknowledgments

This work was supported by KAIA (Korea Agency for Infrastructure Technology Advancement) research project (2014-7AL-003). The authors are grateful to GMVP group for providing the research fund.

#### References

- [1] H. Liang, K.M. Zeng, Research progress on treatment methods of waste water containing dyestuffs, *J. Sichuan Ins. Light Industry Chem. Technol.* 16 (2003) 20–24.
- [2] Y.M. Mao, D.L. Xi, X.B. Yang, Present situation and prospects of the advanced treatment and reuse of dyeing wastewater, *Dyeing Finish.* 8 (2005) 46–48.
- [3] Y.X. Fan, Z.Y. Zhou, Current situation and development prospect of textile dye wastewater treatment methods, *Environ. Prot.* 9 (2002) 22–24.
- [4] K. Dutta, S. Mukhopadhyay, S. Bhattacharjee, B. Chaudhuri, Chemical oxidation of methylene blue using Fenton-like reactions, *J. Hazard. Mater.* 84 (2001) 57–71.
- [5] I.A. Salem, M.S. El-Maazawi, Kinetics and mechanism of color removal of methylene blue with hydrogen peroxide catalyzed by some supported alumina surfaces, *Chemosphere* 41 (2000) 1173–1180.
- [6] B. Jiang, J.T. Zheng, Q. Liu, M.B. Wu, Degradation of azo dye using non-thermal plasma advanced oxidation process in a circulatory airtight reactor system, *Chem. Eng. J.* 204–206 (2012) 32–39.
- [7] M.S. Lucas, J.A. Peres, Decolorization of the azo dye Reactive Black 5 by Fenton and photo-Fenton oxidation, *Dyes Pigm.* 71 (2006) 236–244.
- [8] G. Melin, Treatment Technologies for Removal of Methyl Tertiary Butyl Ether (MTBE) from Drinking Water: Chapter III Advanced Oxidation Processes, National Water Research Institute, 2000.
- [9] S. Haji, B. Benstaali, N. Al-Bastaki, Degradation of methyl orange by UV/H<sub>2</sub>O<sub>2</sub> advanced oxidation process, *Chem. Eng. J.* 168 (2011) 134–139.
- [10] P. Jantawasu, T. Sreethawong, S. Chavadej, Photocatalytic activity of nanocrystalline mesoporous-assembled TiO<sub>2</sub> photocatalyst for degradation of methyl orange monoazo dye in aqueous wastewater, *Chem. Eng. J.* 155 (2009) 223–233.
- [11] W. Glaze, J.W. Kang, D.H. Chapin, The chemistry of water treatment processes involving ozone, hydrogen peroxide and ultraviolet radiation, *Ozone Sci. Eng. J. Int. Ozone Assoc.* 9 (1987) 335–352.
- [12] M. Magureanu, D. Piroi, N.B. Mandache, Degradation of antibiotics in water by non-thermal plasma treatment, *Water Res.* 45 (2011) 3407–3416.
- [13] A.A. Joshi, B.R. Locke, P. Arce, Formation of hydroxyl radicals, hydrogen peroxide and aqueous electrons by pulsed streamer corona discharge, *J. Hazard. Mater.* 41 (1995) 3–30.
- [14] B.R. Locke, M. Sato, Electro hydraulic discharge and non-thermal plasma for water treatment, *Ind. Eng. Chem. Res.* 45 (2006) 882–905.
- [15] M. Li, C.P. Feng, W.W. Hu, Z.Y. Zhang, N. Sugiura, Electrochemical degradation of phenol using electrodes of Ti/RuO<sub>2</sub>-Pt and Ti/IrO<sub>2</sub>-Pt, *J. Hazard. Mater.* 162 (2009) 455–462.
- [16] D.S. Kim, Y.S. Park, Removal of Rhodamine B dye using a water plasma process, *J. Environ. Health. Sci.* 37 (2011) 218–225.

- [17] C. Comninellis, Electrocatalysis in the electrochemical conversion/combustion of organic pollutants for wastewater treatment, *Electrochim. Acta* 39 (1994) 1857–1862.
- [18] M.T. Sulaka, H.C. Yatmazb, Removal of textile dyes from aqueous solutions with eco-friendly biosorbent, *Desalin. Water Treat.* 37 (2012) 169–177.
- [19] S.P. Sun, C.J. Lie, J.H. Sun, S.H. Shi, M.H. Fan, Q. Zhou, Decolorization of an azo dye Orange G in aqueous solution by Fenton oxidation process: Effect of system parameters and kinetic study, *J. Hazard. Mater.* 161 (2009) 1052–1057.
- [20] N.K. Daud, U.G. Akpan, B.H. Hameed, Decolorization of sunzol black DN conc. in aqueous solution by Fenton oxidation process, effect of system parameters and kinetic study, *Desalin. Water Treat.* 37 (2012) 1–7.
- [21] B. Jiang, J.T. Zheng, X. Lu, Q. Liu, M.B. Wu, Z.F. Yan, S. Qiu, Q.Z. Xue, Z.X. Wei, H.J. Xiao, M.M. Liu, Degradation of organic dye by pulsed discharge non-thermal plasma technology assisted with modified activated carbon fibers, *Chem. Eng. J.* 215–216 (2013) 969–978.
- [22] J. Hoigen, H. Bader, Rate constants of reactions of ozone with organic and inorganic compounds in water-II, *Water Res.* 17 (1983) 185–194.
- [23] S.F. Kang, C.H. Liao, S.T. Po, Decolorization of textile wastewater by photo-fenton oxidation technology, *Chemosphere* 41 (2000) 1287–1294.
- [24] M.C. Shih, Kinetics of the batch adsorption of methylene blue from aqueous solutions onto rice husk: Effect of acid-modified process and dye concentration, *Desalin. Water Treat.* 37 (2012) 200–214.
- [25] Y.Z. Zhang, J.T. Zheng, X.F. Qu, Effect of granular activated carbon on degradation of methyl orange when applied in combination with high voltage pulse discharge, *J. Colloid Interface Sci.* 316 (2007) 523–530.
- [26] T. Zhou, X. Lu, J. Wang, Rapid decolorization and mineralization of simulated textile wastewater in a heterogeneous Fenton like system with/without external energy, *J. Hazard. Mater.* 165 (2009) 193–199.
- [27] P. Sunka, Pulse electrical discharges in water and their applications, *Phys. Plasma* 8 (2001) 2587–2594.
- [28] B.D. Soni, J.P. Ruparelia, Decolorization and mineralization of Reactive Black-5 with transition metal oxide coated electrodes by electrochemical oxidation, *Process Eng.* 51 (2013) 335–341.
- [29] M. Gattrell, D.W. Kirk, A study of electrode passivation during aqueous phenol electrolysis, *J. Electrochem. Soc.* 140 (1993) 903–911.